5-2017

Examining the effects of macrophage populations on cancerous tumor growth.

Grace E. Mahlbacher
University of Louisville

Examining the effects of macrophage populations on cancerous tumor growth

By

Grace Mahlbacher
B.S., University of Louisville, May 2016

A Thesis
Submitted to the Faculty of the
University of Louisville
J.B. Speed School of Engineering
as Partial Fulfillment of the Requirements
for the Professional Degree

MASTER OF ENGINEERING

Department of Bioengineering

May 2017

EXAMINING THE EFFECTS OF MACROPHAGE POPULATIONS ON CANCEROUS TUMOR GROWTH

Submitted By:_____
Grace Mahlbacher

A Thesis Approved On

_____
(Date)

By the Following Reading and Examination Committee

_____
Dr. Hermann Frieboes, Thesis Director

_____
Dr. Jill Steinbach-Rankins

_____
Dr. Nihat Altiparmak

ACKNOWLEDGMENTS

I'd like to thank Dr. Hermann Frieboes for his endless patience, mentorship, encouragement, and humor. I had very little experience or confidence in programming before this endeavor, and would not have attempted it without his belief in me.

Thank-you to Dr. Jill Steinbach and Dr. Nihat Altiparmak for taking time out of their busy schedules to be part of my committee.

Special thanks to Louis Curtis for introducing me to the program, and for emergency technical support and wizardry.

Thank-you to Alexandra DeCarlo and Alex Keynton for their pep talks, willingness to lend an ear, and preserving my sanity, and to my parents for their encouragement on my journey towards becoming a professional nerd.

Finally, thank-you to the University of Louisville's Bioengineering Department for an adventurous and enlightening five years.

ABSTRACT

The most abundant immune cell types of the tumor microenvironment macrophages recruited tumor-eluted factors. The role of these immune cells in tumor progression, and the interplay between tumor and immune cells is an emerging field of research with potential for novel treatment strategies. Here, a TIE2 expressing macrophage (TEM) subtype is integrated into a virtual tumor model. Within the 2D microenvironment, the TEM will differentiate from an extravasated monocyte precursor, congregate around the abluminal side of the vasculature in response to a chemoattractant gradient, secrete cytokines which favor differentiation of a separate angiogenic macrophage subtype [1]. The effects of macrophage populations on tumor progression on angiogenic activity and tumor growth will be examined.

TABLE OF CONTENTS

NOMENCLATURE

M1 = tumoricidal macrophage subtype
M2 = tumorigenic macrophage suntype
TEM = TIE2-expresseing (angiogenic) macrophage subtype
TAM = Tumor-Associated Macrophage
$M\phi$ = Monocyte (macrophage precursor)
TAF = Tumor Angiogenisis Factor
Ang2 = Angiopoietin2
IL-10 = Interleukin 10
NO = Nitric oxide
VEGF = Vascular Endothelial Growth Factor

LIST OF TABLES

LIST OF FIGURES

I. INTRODUCTION

A. Background on Tumor-Associated Macrophages

The role of tumor-associated macrophages (TAMs) in tumor growth (Guo, Buranych et al. 2013, Chanmee, Ontong et al. 2014, Guo, Buranych et al. 2014, Tripathi, Tewari et al. 2014) and treatment response (Squadrito and De Palma 2011, De Palma and Lewis 2013) has been the subject of increased study in the past several years. What has emerged is that populations of tumor-associated macrophages are diverse in both phenotype and lineage (Laoui, Movahedi et al. 2011, Italiani and Boraschi 2014). While an increased presence of macrophages at a tumor lesion site is generally correlated with poor prognosis, within the phenotypic range of TAMs are subtypes that produce various and even opposing roles in tumor progression (Chanmee, Ontong et al. 2014) (Roca, Varsos et al. 2009). The range of tumorigenic and tumoricidal phenotypes reflects the conflicting cues within the tumor environment. While the immune response to tumor growth may begin as primarily tumoricidal, with macrophages of the M1 or classically activated type targeting tumor cells, cytokines secreted by the tumor exploit the

relatively fluid phenotype of the TAMs to promote tumor growth and survival (Yuan, Hsiao et al. 2015) via the M2 subtype.

A third, more recently discovered subtype, the TIE-2 receptor expressing macrophage (TEM), develops from a distinct monocyte precursor, and displays unique and non-redundant behaviors highly relevant to tumoral angiogenesis (De Palma, Murdoch et al. 2007, Lewis, De Palma et al. 2007, Venneri, Palma et al. 2007, De Palma, Venneri et al. 2008). In particular, the critical role of TEMs in tumor angiogenesis and vascular remodeling (De Palma, Murdoch et al. 2007, Lewis, De Palma et al. 2007, Venneri, Palma et al. 2007, De Palma, Venneri et al. 2008, Riabov, Gudima et al. 2014, Stockmann, Schadendorf et al. 2014) was shown by increased TEM infiltration following administration of anti-angiogenic agents (Welford, Biziato et al. 2011) as well as the blocking of the angiogenic factor Angiopoietin-2 (ANG2), a TIE2 ligand associated with activated endothelial cells. This lead to regression of tumor vasculature and arrested tumor progression (Mazzieri, Pucci et al. 2011).

B. Background on Macrophage Subtypes

The M1 extreme of the macrophage activation spectrum is commonly associated with inflammatory responses and tumoricidal activity by release of proinflammatory cytokines and oxygen species such as nitric oxide (NO), which encourage tumor cell apoptosis (Plank and Sleeman 2003) (Edin, Wikberg et al. 2012). Its presence in the tumor microenvironment is correlated with reduced angiogenesis required to supply the increased tumor metabolic needs, and thus reduced tumor growth and survival (Yuan,

Hsiao et al. 2015) (Italiani and Boraschi 2014). The relative proportion of the M1 macrophages generally decreases with tumor progression. The M1 subtype is identified by surface receptors $CD14^{++}CD16^{-}$ (Plank and Sleeman 2003).

The M2 or alternatively activated macrophages encompass a broader family of macrophages involved in tissue healing under normal conditions. Within the tumor microenvironment, they are recruited for tumor progression (Chanmee, Ontong et al. 2014), and generally comprise a larger portion of the TAMs in advanced tumors (Sica and Mantovani , Chanmee, Ontong et al. 2014). Hypoxia-induced factors such as VEGF-A, endothelin-2, and interleukin-10 secreted in the tumor environment encourage differentiation towards the M2 phenotype (Murdoch, Giannoudis et al. 2004). Within the tumor microenvironment, M2s secrete factors such as TGF-β1 which facilitates cancer cell proliferation (Leonard, Curtis et al. 2016) (Italiani and Boraschi 2014), VEGF-A which promotes angiogenesis and recruits additional macrophages, and MMP-9 which facilitates angiogenesis by degrading the extracellular matrix (Chanmee, Ontong et al. 2014). The proportion of M2 macrophages in the microenvironment tends to increase with tumor progression. The M2 subtype is identified by surface receptors $CD14^{dim}CD16^{+}$ (Italiani and Boraschi 2014).

TIE2 expressing macrophages (TEMs) are a tumorigenic subtype upregulated in a variety of environments where angiogenesis occurs, including tumor lesions (Matsubara, Kanto et al. 2013) and for post-ischemic recovery (Patel, Smith et al. 2013). They have been found in breast cancer metastatic lymph nodes (Kim, Kang et al.), and in colorectal metastases to the liver (Catarinella, Monestiroli et al.). They can be identified by the expression of the TIE2 receptor on their surface which, curiously, is also expressed by

blood vessel endothelial cells, where they are integral to angiogenic pathways and development (Plank and Sleeman 2003, Matsubara, Kanto et al. 2013). Recent research indicates that TEMs are recruited to the tumor microenvironment at an early phase of development. There, they are believed to play a pivotal role in tumor neovascular development by activating the "angiogenic switch" – a transition that occurs when a tumor begins to recruit nearby vasculature to supply its increased metabolic demands (De Palma and Naldini 2011).

C. Specific Roles of TEMs

The chief contribution of TEMs to tumor progression appears to be facilitation of angiogenesis through structural and paracrine support. The macrophage's eponymous receptor, TIE2, binds the growth factors angiopoietin 1 and 2. In addition to having a direct chemotactic effect on the TEMs (Coffelt, Tal et al. 2010) interactions with angiopoietins lead to the upregulation of several factors necessary to angiogenic processes, including MMP-9, CTSB, and IL-10, not dissimilar to role of the M2 subtype (Coffelt, Tal et al. 2010, Coffelt, Chen et al. 2011). However, TEMs have a more multifaceted involvement in angiogenesis (De Palma, Venneri et al. 2008). In addition to upregulating these factors in TEMs, angiopoietin 2 (Ang2) acts as a chemoattractant, causing the TEMs to congregate along the abluminal side of vessels (Lewis, De Palma et al. 2007). Here, TEMs are thought to directly facilitate vessel sprouting by providing both a structural scaffold and paracrine support for endothelial sprouts, aiding in their growth (De Palma, Murdoch et al. 2007), and preventing collapse due to the high hydrostatic pressure associated with the tumor microenvironment (Matsubara, Kanto et al. 2013). As

a tumor grows and its metabolic needs increase, TEMs continue to fill a supportive role in the growth and maturation of the neovasculature that supplies it with nutrients and oxygen (Matsubara, Kanto et al. 2013) . In a 2008 study by De Palma et al. comparing a tumor model with an intact and TEM-knockout population of tumor associated macrophages, the tumors with an intact population showed just under a four-fold increase in vascular development in comparison to the TEM-ablated population (De Palma, Venneri et al. 2008).

In addition to their more direct roles in facilitating neovascular development, TEMs also contribute to the cocktail of other tumor-friendly cytokines in the microenvironment. IL-10 is an immune cytokine secreted from most leukocytes, including macrophages, as well as tumor cells themselves (Hamidullah, Changkija et al. 2012). It has pleiotropic effects in the tumor microenvironment, being implicated in both suppression of tumorigenic cytokines such as IL-6 [31], and in improved immune escape, poor prognosis, and advanced cancer stage (Kozlowski, Zakrzewska et al. 2003, Dehqanzada, Storrer et al. 2007, Esquivel-Velazquez, Ostoa-Saloma et al. 2015, Capone, Guerriero et al. 2016). While it is known to be upregulated in several cancer types, including breast cancer (Beckebaum, Zhang et al. 2004, Esquivel-Velazquez, Ostoa-Saloma et al. 2015) a consensus has yet to be reached on whether it is a definitive indicator of tumor progression and patient prognosis, as some studies have suggested that its overexpression leads to subsequent immune rejection of the tumor (Mocellin, Marincola et al. 2005). IL-10 is also known to play a role in inducing infiltrating monocytes to adopt the tumorigenic M2 phenotype (Italiani and Boraschi 2014). TIE2-

expressing macrophages are known to secrete IL-10, and thus may contribute to the increased ratio of M2 to M1 macrophages in the tumor microenvironment.

D. Contribution to Previous Models

Previous mathematical modeling work has explored critical aspects of tumor-associated macrophage activity. Owen and Sherratt (Owen and Sherratt 1998, Owen and Sherratt 1999) presented a model in which macrophages entered the tumor environment to selectively target tumor cells. Later models were developed to simulate macrophages primed to destroy cancer cells on contact (Byrne, Cox et al. 2004) or by drug delivery (Owen, Byrne et al. 2004). In (Webb, Owen et al. 2007) it was shown that effective macrophage targeting of hypoxic tumor cells would benefit from non-cell-cycle dependent drugs or limited-diffusivity. In (Owen, Stamper et al. 2011) it was found that the combination of conventional and macrophage-based therapies using magnetic nanoparticles could be synergistic. In (Chen, Bobko et al. 2014) the role of tumor macrophage hypoxia inducible factors (HIFs) in chemotherapy effectiveness was evaluated. Recently, a model exploring the efficacy of nanoparticle albumin-bound-paclitaxel (nAb-PTX) using macrophages in a multistage vector system as a therapy for hypervascularized breast cancer metastases in the liver was developed (Leonard, Curtis et al. 2016).

The interplay of the various monocyte subtypes with the changing tumor microenvironment presents a relevant and challenging task which may benefit from a systems analysis perspective. To this end, recent mathematical modeling and

computational simulation work (Leonard, Curtis et al.) has evaluated the role of macrophages in the tumor microenvironment to gain insight into implications for cancer treatment and drug delivery. In this study, a computational framework to further evaluate the role of TEMs in relation to M1 and M2 macrophage phenotypes on the growth of vascularized tumor lesions is developed.

III. PROCEDURE

The computational model builds upon recent work simulating generic tumor-associated macrophages (TAMs) in a vascularized tumor environment (Leonard, Curtis et al. 2016), in which a breast cancer lesion metastasized to the liver was simulated – in an microenvironment that is known to favor the recruitment of TAMs (Bocuk, Krause et al. 2015). In (Leonard, Curtis et al. 2016), macrophages were utilized as a drug vector, and their performance was evaluated experimentally and via computational simulation. Here, we do not assume that drug is vectored by macrophages, and instead focus on the effects of various macrophage population subtypes on the tumor lesion progression.

Briefly, the model is composed of a tumor lesion in a 2D grid of preexisting vasculature as previously described (Macklin, McDougall et al. 2009, van de Ven, Wu et al. 2012, Wu, Frieboes et al. 2013, Leonard, Curtis et al. 2016). Two types of macrophage subtypes are defined – the M1 and M2. The TEM subtype is added as a third population that promotes angiogenesis for tumors in the liver (Matsubara, Kanto et al.). Given that the monocytes are not biologically active in the model, a simplifying assumption is made that TIE2 expressing macrophage differentiate from the same monocyte precursor as the M1 and M2 macrophage subtypes. As the TEM phenotype appears in the environment, its effects are modeled as follows:

- Increasing differentiation of TIE2 macrophages from a monocyte precursor with tumor progression
- Semi-stochastic movement of TEMs along a chemoattractant gradient (Ang2) secreted by the peritumoral vasculature, as well as monocyte attractant from the hypoxic regions of the tumor.
- The protein released by the TEMs is modeled after IL-10 to examine the effects of cytokine release in the context of immunomodulatory activity.
- Increased M2 differentiation in response to TEM-eluted IL-10 in the system
- Increased angiogenesis and resilience of tumoral neovasculature

The relevant model parameters are outlined in Table I.

TABLE I

MACROPHAGE-ASSOCIATED PARAMETERS.

Parameter Description	Value	Reference
Physiological Parameters		
% of macrophages per tumor total cells	10%	Calibrated to match (Leonard, Curtis et al. 2016)
TEM-driven tumor neovasculature increase	~4-fold	(De Palma, Venneri et al. 2008)
TEM portion of differentiated macrophages	55-70%	(Venneri, Palma et al. 2007)
M2/M1 ratio in highly metastatic tumors	2.06	(Cui 2013)
M2/M1 ratio in moderately metastatic tumors	0.77	(Cui)

A. Tumor Growth

The tumor growth model is based on Macklin et al. (Macklin, McDougall et al. 2009) and builds upon (Wu, Frieboes et al. 2013, Leonard, Curtis et al. 2016).

Simulation of tumor growth begins with a small lesion in a 2D grid of blood vessels representing a regularly-spaced capillary grid. The tumor progression is modeled in discrete time increments; the tumor conditions are evaluated, updated, and recorded every 0.075 days. Advection of the tumor and advancement of its boundary are subject to changes in the microenvironment such as fluid pressure, diffusion of hypoxic proteins and other angiogenic factors, and concentration of oxygen, glucose and other vital nutrients (here, simplified as oxygen only). Altogether, the tumor microenvironment may be described in four regions based on oxygen and proliferation levels. These are:

- Necrotic region, ΩN, in which oxygen levels are insufficient for viability.
- Hypoxic region, ΩH, in which oxygen levels are sufficient for viability but not proliferation.
- Proliferating region, ΩP, in which oxygen levels are sufficient for proliferation.
- Normal (non-tumoral) tissue.

Tumor boundary advancement with velocity V_c through the porous extracellular matrix of the surrounding normal tissue is based on Darcy's law (Macklin, McDougall et al. 2009):

$$V_c = -\mu \nabla P + \chi_E \nabla E \quad (1)$$

where μ is tissue mobility, encompassing the roles of cell-cell and cell-matrix adhesion, P is oncotic pressure, χ_E is haptotaxis, and ∇E is the density of the extracellular matrix. Cell

density in the proliferating region is constrained to a value at or below 70% of the tumor volume, with extracellular matrix comprising the remaining volume.

Via a simplifying assumption of uniform density E in the proliferating tumor region, the relationship between velocity change and tumor growth is (Macklin, McDougall et al. 2009):

$$\nabla \cdot V_c = \lambda_p \tag{2}$$

where λ_p is the non-dimensionalized net tumor proliferation rate (described below).

As oxygen falls below the threshold for a proliferation state in regions distant from vasculature, hypoxic tissue regions develop and release tumor angiogenic factor (TAF) and other factors (see Table II).

TABLE II

CHEMOKINE CHARACTERISTICS

Chemokine	**Function**	**Source**	**MW (Da)**	**Fraction of TAF Diffusivity**
M1f	M1 differentiation	Proliferating & hypoxic tumor cells	21000	1
M2f	M2 differentiation	Proliferating & hypoxic tumor cells	18606	3.7606
IL-10	TEM-eluted factor	TEM	18606	3.7606
T2f	TEM differentiation	Proliferating & hypoxic tumor cells	60179	1
Ang2	TEM chemoattractant	Neovasculature	~70000	0.26591

TAF diffuses outward through the tumor and into the surroundings, where it triggers endothelial cell sprouts in the peritumoral vascular grid. Additionally, TAF triggers extravasation of macrophages, analogous to the action of VEGF on macrophage recruitment to the tumor (Lewis and Murdoch , Hsu, Poché et al.). If oxygen falls below a vital threshold, necrotic tissue develops within the tumor and degrades. The tumor model main parameters are shown in Table III.

TABLE III

MAIN PARAMETERS AND ASSOCIATED VALUES

Parameter	**Value**	**Reference**
Tumor native mitosis rate	0.5 day^{-1}	Estimated
Tumor tissue threshold for hypoxia	0.5750	Calibrated to match (Leonard, Curtis et al. 2016)
Tumor tissue threshold for necrosis	0.5325	Calibrated to match (Leonard, Curtis et al. 2016)
Oxygen diffusivity	1 (*)	(Wu, Frieboes et al. 2013)
Oxygen transfer rate from vasculature	5 (*)	(Wu, Frieboes et al. 2013)
Oxygen uptake rate by proliferating tumor cells	1.5 (*)	(Wu, Frieboes et al. 2013)
Oxygen uptake rate by hypoxic tumor cells	1.3 (*)	(Wu, Frieboes et al. 2013)
Oxygen uptake rate by tumor microenvironment	0.12 (*)	(Wu, Frieboes et al. 2013)
Oxygen decay rate	0.35 (*)	(Wu, Frieboes et al. 2013)

Note: (*) value is rescaled by the square of the simulation system characteristic length (1 cm) and divided by the system characteristic time (1 sec) multiplied by the oxygen diffusivity (Nugent and Jain) (1 x 10-5 cm2 s-1).

B. Angiogenesis and Vascular Development

The angiogenesis model, simulating the model by (McDougall, Anderson et al. 2006) and based on (Macklin, McDougall et al. 2009, Wu, Frieboes et al. 2013), outlines the mechanical and chemical effects of tumor proliferation on the growth, maturation, flow, flux, and collapse of the surrounding vasculature. The vasculature is simplified to a grid, from which irregular vessels sprout and grow in response to gradients of factors and pressures produced by the tumor tissue.

Each vessel sprout grows semi-stochastically, with the probability of growing in four directions weighted by the presence of TAF gradient produced by ΩH. The sensitivity of the vascular growth is increased in response to contact with factors secreted by the TEMs. The magnitude of this response is tuned to correlate with the four-fold increase in vasculature surface area found to result from TEM-eluted factors by De Palma et al (De Palma, Venneri et al. 2008).

The change ΔR in radii R of the vessels are modeled according to pressures imposed by the fluid carried within them (Pries, Secomb et al. 1998, McDougall, Anderson et al. 2002, McDougall, Anderson et al. 2006, Macklin, McDougall et al. 2009),

$$\Delta R = \left(S_{wss} + S_p + S_m - S_s\right)R \tag{3}$$

where S_{wss} is the local wall shear stress stimulus, S_p is the intravascular pressure stimulus, S_m is the flow carrying hematocrit stimulus, and S_s is the natural shrinking

tendency of the vessel as a result of the properties of the basal lamina. This natural shrinking tendency is a constant value S_s (Pries, Hopfner et al. 2010) unless the pressure PC within the vessel reaches a critical pressure P_{CT}, at which point the shrinking tendency increases proportionally to the pressure with a rate k_{pc} to simulate complete vessel collapse. Vessels may partially recover if the stress is relieved (Wu, Frieboes et al. 2013):

$$S_s = k_s \qquad if\ P_C \leq P_{CT} \tag{4}$$

$$S_s = k_s + k_{pc}(P_c - P_{CT}) \qquad if\ P_C > P_{CT} \tag{5}$$

In the model, the effect of TEM proximity at a given location is incorporated to provide a protective effect on the neovasculature. Specifically, if a TEM is at an adjacent location on the matrix to the blood vessel, $\mathbf{1}_{\text{TEM}}$ is 1, and $\mathbf{1}_{\text{TEM}}$ is 0 if there is no TEM present. The factor $k_{abluminal}$ has the effect of greatly reducing the natural shrinking tendency of the vessel (see Table IV). The change in radius therefore is (Macklin, McDougall et al. 2009):

$$\Delta R = \left(S_{wss} + S_p + S_m - S_s(1 - k_{abluminal}\mathbf{1}_{TEM})\right)R\Delta t \tag{6}$$

TABLE IV

ANGIOGENESIS COEFFICIENTS

$k_{abluminal}$	Effect of abluminal TEM	10E-5	Calibrated to match (Lewis, De Palma et al. 2007)
k_s	Natural shrinking tendency of the vessel	2.24	(Wu, Frieboes et al. 2013)

C. Macrophages

Following (Leonard, Curtis et al. 2016), macrophages are simulated to extravasate in proportion to the local concentration of macrophage chemoattractants (e.g., pro-angiogenic factors), and to preferentially migrate towards tissue regions (e.g., hypoxic tissue or vascular sprouts) along the increasing gradient of these chemoattractants.

1. Effects on Tumor Growth

The effects of macrophage variants M1 and M2 are characterized by the action of their associated tumoricidal and tumorigenic nitric oxide (NO) and tumor growth factors, respectively. This is simulated by the M2 subtype favoring tumor growth by lowering the oxygen threshold for tissue to become necrotic while the M1 subtype counters this effect by secreting NO, which results in tumor tissue death.

The tumor growth factor secreted by the M2 macrophages achieves a transient local lowering of the viable oxygen threshold – the oxygen level below which tumor cells die – as follows:

$$Q_{OL\,f} = \lambda_{OL} \cdot (1 - M2_{GF}) \cdot (\bar{Q}_{OL} - Q_{OL\,i}) - \lambda_{GF} \cdot M2_{GF} \cdot (Q_{OL\,i} - Q_{OL\,min}) \quad (7)$$

where $Q_{OL\,f}$ is the final quiescence oxygen level, λ_{OL} is the recovery rate of $Q_{OL\,f}$ to the standard quiescence oxygen level $\bar{Q}_{OL}$, $Q_{OL\,i}$ is the initial quiescence oxygen level, $M2_{GF}$

is the local presence of M2 growth factor, λ_{GF} is the M2 growth factor effect rate, and $Q_{OL\,min}$ is the lower bound of the quiescence oxygen level (see Table V)

In addition to inhibiting tumor death, the presence of the M2 growth factor has a positive effect on the proliferating region as follows:

$$\lambda_{M2GF\,f} = M2_{GF} \cdot P_{M2GF} \cdot (0.5 - \lambda_{M2GF\,i}) - \lambda_{rec} \tag{8}$$

where $\lambda_{M2GF\,f}$ is the final proliferation rate due to the M2 growth factor, P_{M2GF} is the M2 growth factor proliferation effect, $\lambda_{M2GF\,i}$ is the initial proliferation rate due to the M2 growth factor, and λ_{rec} is the recovery rate of λ_{M2GF} to zero (see Table V).

The NO produced by the M1 subtype is incorporated directly into the proliferation term as follows:

$$\lambda_p = \begin{cases} non\ tumoral: & 0 \\ \Omega_P: & (\lambda_M + \lambda_{M2GF}) \cdot C_{O2} - M1_{NO} \cdot \mathbf{1}_{M1} - \lambda_A \\ \Omega_H: & \lambda_{M2GF} \cdot C_{O2} - M1_{NO} \cdot \mathbf{1}_{M1} - \lambda_A \\ \Omega_N: & -G_N \end{cases} \tag{9}$$

where λ_M is the tumor native mitosis rate, C_{O2} is the local oxygen concentration, λ_A is the apoptosis rate due to natural tumoral cell death, $M1_{NO}$ is the effect of nitric oxide, and 1_{M1} is the presence of an M1 macrophage at that location. $G_N$is the non-dimensionalized rate of cell degradation in the necrotic region (see Table V).

TABLE V

MACROPHAGE EFFECTS ON TUMOR GROWTH

$\bar{Q}_{OL}$	Quiescence oxygen level upper bound	0.5750	
$Q_{OL\,min}$	Quiescence oxygen level lower bound	0.5325	
λ_{OL}	Recovery rate of quiescent oxygen level	0.05(*)	(Wu, Frieboes et al. 2013)
λ_{GF}	M2 growth factor effect rate	200(*)	(Wu, Frieboes et al. 2013)
P_{M2GF}	M2 growth factor proliferation effect coefficient	1000	(Wu, Frieboes et al. 2013)
λ_{rec}	Recovery rate of λ_{M2GF} to zero	0.1(*)	(Wu, Frieboes et al. 2013)
$M1_{NO}$	Effect of nitric oxide coefficient	1.5	Calibrated to match (Yuan, Hsiao et al. 2015)
G_N	Rate of cell degradation for the necrotic region.	0.3(*)	(Wu, Frieboes et al. 2013)

Note: (*) Value is rescaled by the square of the simulation system characteristic length (1 cm) and divided by the system characteristic time (1 sec) multiplied by the oxygen diffusivity (Nugent and Jain) (1 x 10-5 cm2 s-1).

2. Differentiation

Given the increased ratio of M2/M1 macrophages typical of tumor lesions, the role of TEM-produced IL-10 on the ratio of M2/M1 macrophage subtypes is modeled. A target range of 0.32-5.23 was used, to match in vitro data for metastatic tumors in the liver (Cui 2013).

As monocyte precursors $M\phi$ extravasate from the vasculature in the tumor region, they come into contact with proteins diffusing from the tumor interior and vasculature that influence their differentiation. The concentration of factors encouraging differentiation of given subtypes, analogous to interleukins and angiopoietins, influences the differentiation rate for each subtype modeled. The rate is dependent on the size of the interval that a randomly generated number may fall into, as follows:

$$M\phi = \begin{cases} M1: & k_{M1} \cdot C_{M1f} \\ M2: & k_{M2} \cdot (C_{M2f} + k_{T2M2} \cdot C_{IL-10}) \\ TEM: & \left(k_{T2} \cdot C_{T2f} + k_{Ang2} C_{Ang2}\right) \end{cases} \quad (10)$$

where k_{M1}, k_{M2}, k_{T2} are intensity coefficients tuned to reflect the relative prevalence of M1 or M2 differentiating monocytes and TIE2 expressing monocytes infiltrating the tumor, C_{M1f}, C_{M2f}, C_{IL-10}, C_{T2f} and C_{Ang2} are local concentrations of chemokines and other factors favorable to M1, M2, or TEM differentiation, and k_{Ang2} and k_{T2M2} are intensity coefficients to tune the effect of Ang2 and Il-10 favoring M2 differentiation, respectively. The values of macrophage-associated variables and coefficients are defined in Table VI.

TABLE VI

MACROPHAGE DIFFERENTIATION SCALING COEFFICIENTS

k_{M1}	Differentiation of M1 macrophage	20	(Leonard, Curtis et al. 2016)
k_{M2}	Differentiation of M2 macrophage	11	(Leonard, Curtis et al. 2016)
k_{T2}	Differentiation of TEM	1.5	(Venneri, Palma et al. 2007)
k_{Ang2}	Effect of Ang2 on TEM differentiation	0.95	Calibrated to match (Venneri, Palma et al. 2007, Chanmee, Ontong et al. 2014)
k_{T2M2}	Effect of IL-10 on M2 differentiation	0.055	Calibrated to match (Venneri, Palma et al. 2007) (Cui 2013)

The concentration of IL-10 in pg/mL is calculated by treating each pixel in the spatial model as a 3-dimensional voxel. Thus, the final concentration for IL-10 in simulations with the TEM subtype present are within observed values of 5.6-37 pg/mL for breast cancers of various TNM stages (Kozlowski, Zakrzewska et al. 2003). The

exception is a model without the M2 subtype, which achieved reduced tumor and vascular growth (see Table VII).

TABLE VII

IL-10 CALCULATIONS

Variation	IL-10 Units	Daltons	pg	Voxel Area (mm^3)	IL-10 Concentration (pg/mm^3)	IL-10 Concentration (pg/mL)
M1 M2 TEM	8201.43	152598185	0.000253395	0.04	0.00633488	6.3349
M2 TEM	7867.44	146383870	0.000243076	0.04	0.00607691	6.0769
M1 TEM	6978.27	129839715	0.000215604	0.04	0.00539010	5.3901
TEM	8276.8	154000560	0.000255724	0.04	0.00639310	6.3931

3. Chemokine Production and Diffusion

Assuming steady-state conditions, the overall mass balance for a particular chemokine *C* is [62]:

$$0 = \nabla \cdot (D_C \nabla C) + \bar{\lambda}^C_{production}(1-C)\mathbf{1}_\Omega - \bar{\lambda}^C_{circulation}\mathbf{1}_{vessel} - \bar{\lambda}^C_{decay}C \quad (11)$$

where D_C is diffusivity and $\bar{\lambda}^C_{production}$, $\bar{\lambda}^C_{circulation}$, and $\bar{\lambda}^C_{decay}$ are the (constant) rates of chemokine production, wash-out via circulation, and decay, respectively.

For all the diffusion equations, as well as the pressure and angiogenic factors, the conditions at the boundaries are (zero Neumann condition), where N is the element at the boundary (oxygen, pressure, or chemokine).

4. Movement

Monocytes as well as M1 and M2 macrophages migrate through the interstitium guided by gradients of oxygen, pressure, and chemoattractants. Movement in one of four directions is determined semi-stochastically, similar to the differentiation algorithm above. The probability of movement in the x+1 direction is as follows:

$$P_{x+1} = (M_O \cdot \Delta O_{x+1} + M_P \cdot \Delta P_{x+1} + M_C \cdot \Delta Chemo_{x+1}) \quad (12)$$

where M_O, M_P and M_C are intensity coefficients for the influence of oxygen concentration, pressure, and chemoattractant on macrophage movement (see Table), and $\Delta O_{x+1}, \Delta P_{x+1}$ and $\Delta Chemo_{x+1}$ are the difference in concentration of the factor of interest from the current point to the direction in question. The same calculations are made for the remaining three directions in the 2D Cartesian grid. A random number is then generated which may fall into the interval calculated for one of these four directions. Otherwise, the macrophage remains in place.

The method of movement for the TEM is also semi-stochastic, but relies upon a different chemoattractant – Ang2 gradients secreted by the neovasculature. The probability of movement in the x+1 direction is modeled as follows:

$$P_{x+1} = M_{Ang2} \cdot \Delta Ang2_{x+1} \quad (13)$$

where M_{Ang2} is the intensity coefficient tuned to scale the response of TEMs to the Ang2 concentration gradient in each direction.

TABLE VIII

MACROPHAGE MOVEMENT SCALING COEFFICIENTS

M_O	Effect of oxygen on macrophage movement	1000	(Leonard, Curtis et al. 2016)
M_P	Effect of oxygen on macrophage movement	500	(Leonard, Curtis et al. 2016)
M_C	Chemotactic macrophage movement	350	(Leonard, Curtis et al. 2016)
M_{Ang2}	Effect of Ang2 on TEM movement	1000	Calibrated to match (De Palma and Naldini 2011)

Note: (*) Value is rescaled by the square of the simulation system characteristic length (1 cm) and divided by the system characteristic time (1 sec) multiplied by the oxygen diffusivity (Nugent and Jain) (1 x 10-5 cm2 s-1).

D. Numerical Methods

A detailed description of the numerical methods employed in the model is given in (Wu, Frieboes et al.) and Macklin (Macklin, McDougall et al.) and their incorporated references. The continuous equations governing gradients of oncotic pressure by which the tumor advances, as well as diffusion of oxygen, TAF, chemokines, and other factors are applied to a discrete 2D Cartesian grid via backward Euler's method with centered finite difference calculations. Discretization of the change in pressure at the boundary between oncotic and normal tissue, an immersed moving boundary with jump boundary conditions, is applied by a ghost cell method described in (Macklin and Lowengrub) .

The resulting discretized equations are then solved to steady state at time steps of 0.075 days (Wu, Frieboes et al.) according to a nonlinear adaptive Gauss-Seidel iteration method (Macklin and Lowengrub , Macklin and Lowengrub) to produce, at each grid

location, values for concentrations of diffusible factors, oncotic pressure, and interstitial fluid pressure outside the tumor.

To map the changing curved topology of the boundaries between tumor hypoxic/normoxic regions and tumor and normal tissue, the level set method is used. The vessel radii calculated at each iteration influence the blood flow, which in turn modulates the hematocrit in the angiogenesis component, which affects the extravasation of monocytes and oxygen from the vasculature. The monocytes and macrophages in (Leonard, Curtis et al.) were originally modeled as point sources of drug. In this instance, macrophages do not release active drug into the system, but rather IL-10, M2GF, and NO. The monocytes are not biologically active in this model.

RESULTS

The tumor, vascular, and macrophage parameters were calibrated as described above. The single and combined effects of the three macrophage types on tumor growth were then evaluated, as described in the following table:

TABLE IX

SUMMARY OF MACROPHAGE CASES EVALUATED

Variation 1	Variation 2	Variation 3	Variation 4	Variation 5	Variation 6	Variation 7	Variation 8
M1		M1	M1			M1	
M2	M2	M2		M2			none
TEM	TEM				TEM	TEM	

A case to match *in vivo* macrophage ratios was first run, with all three macrophage subtypes present (Variation 1). The other cases then examined the tumoral response to other population variants. Variation 2 and 5 represent worst-case subtype populations – the tumorigenic subtype M2 or M2 and TEM only, driving unrestrained tumor growth. Variation 3 is the TEM-ablated model, utilizing M1 and M2 only. Variation 4 is the best-case population, with the tumoricidal subtype M1 only.

Variation 6 examined the vascular protective effects of TEM alone without its effects on M1 and M2 populations. Variation 4 utilizes the tumoricidal subtype M1 and immunomodulatory TEM only. Finally, macrophage activity is entirely absent in Variation 8, providing a baseline tumor growth profile.

Each was observed over a simulated 13.5-day timespan of tumor growth.

A. Interaction with blood vessels

Following the Ang2 gradient secreted by the neovasculature (Fig. 1, bottom right panel), the TEMs in variations 1, 2, 4, and 7 preferentially clustered around angiogenic vessels (Fig. 1, middle right panel). Here, they prevented vessel collapse due to the increased pressure of the tumor environment (Fig. 1, top middle panel) as expressed in Equation 6.

The extravasation of monocytes and subsequent macrophage differentiation is triggered by the release of TAF from the hypoxic interior of the tumor (Fig. 1, bottom left panel). This first occurred when the lesion reached 200 μm in diameter (Day 7.35 of growth). All four models had the same tumoral and vascular growth pattern until this time, whereupon they began to diverge.

Fig. 1 provides a representative assessment of tumor growth, vascular development, macrophage infiltration, and key secreted factors at 13 days post-inception in Variation 1.

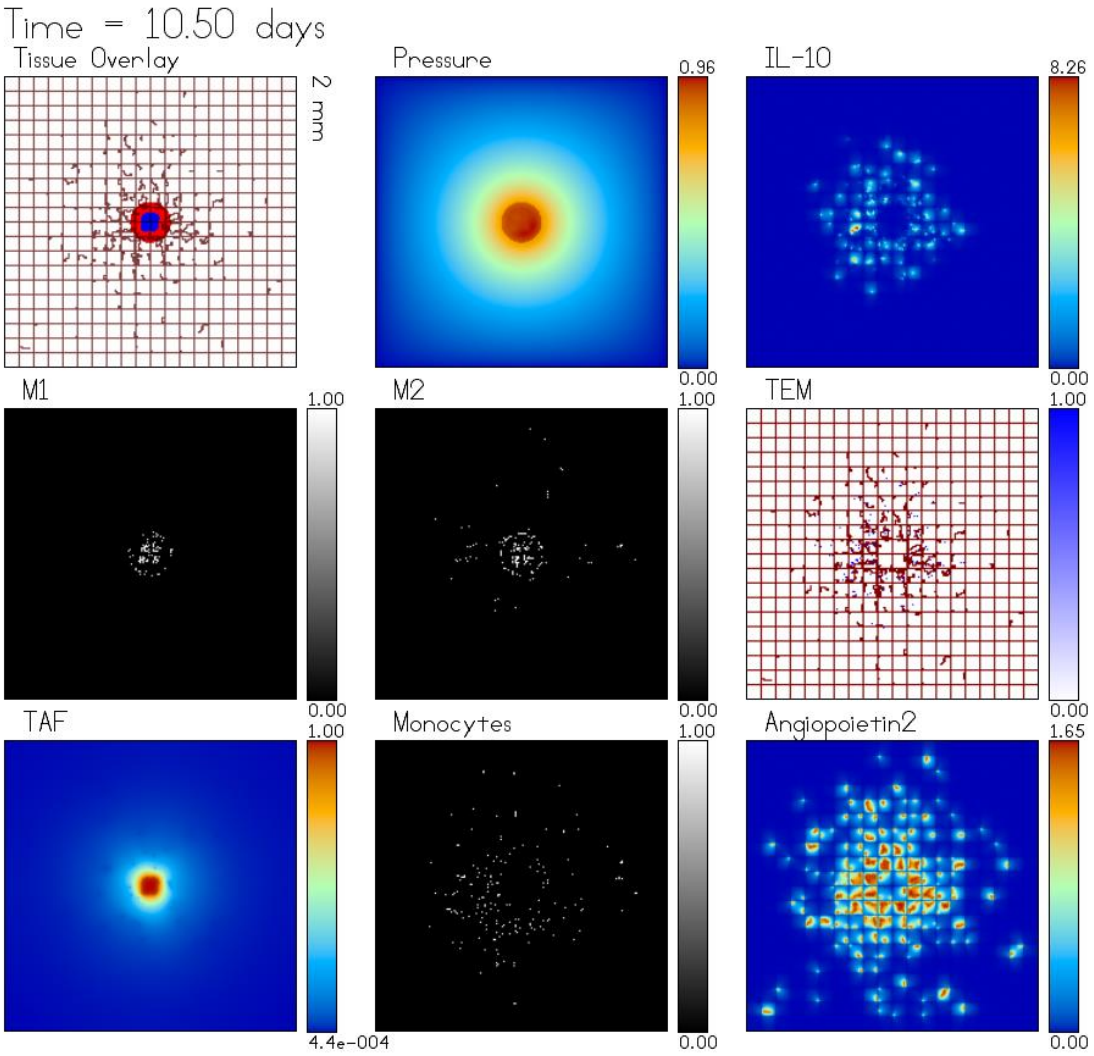

FIGURE 1 – REPRESENTATIVE ASSESSMENT OF TUMOR GROWTH

B. Macrophage ratios

The effect of the TEM subtype on macrophage differentiation can be observed in where the M1 and M2 subtypes are clustered. The M1 subtypes are mostly concentrated within the tumor lesion, while the M2 subtypes are in the immediate periphery as a consequence of the monocyte contact with IL-10 eluted from TEMs (see Fig.1, top right panel, and Fig 2.). The TEM subtypes cluster around angiogenic vessel sprouts as a result of the Angiopoietin2 secreted by the neovasculature.

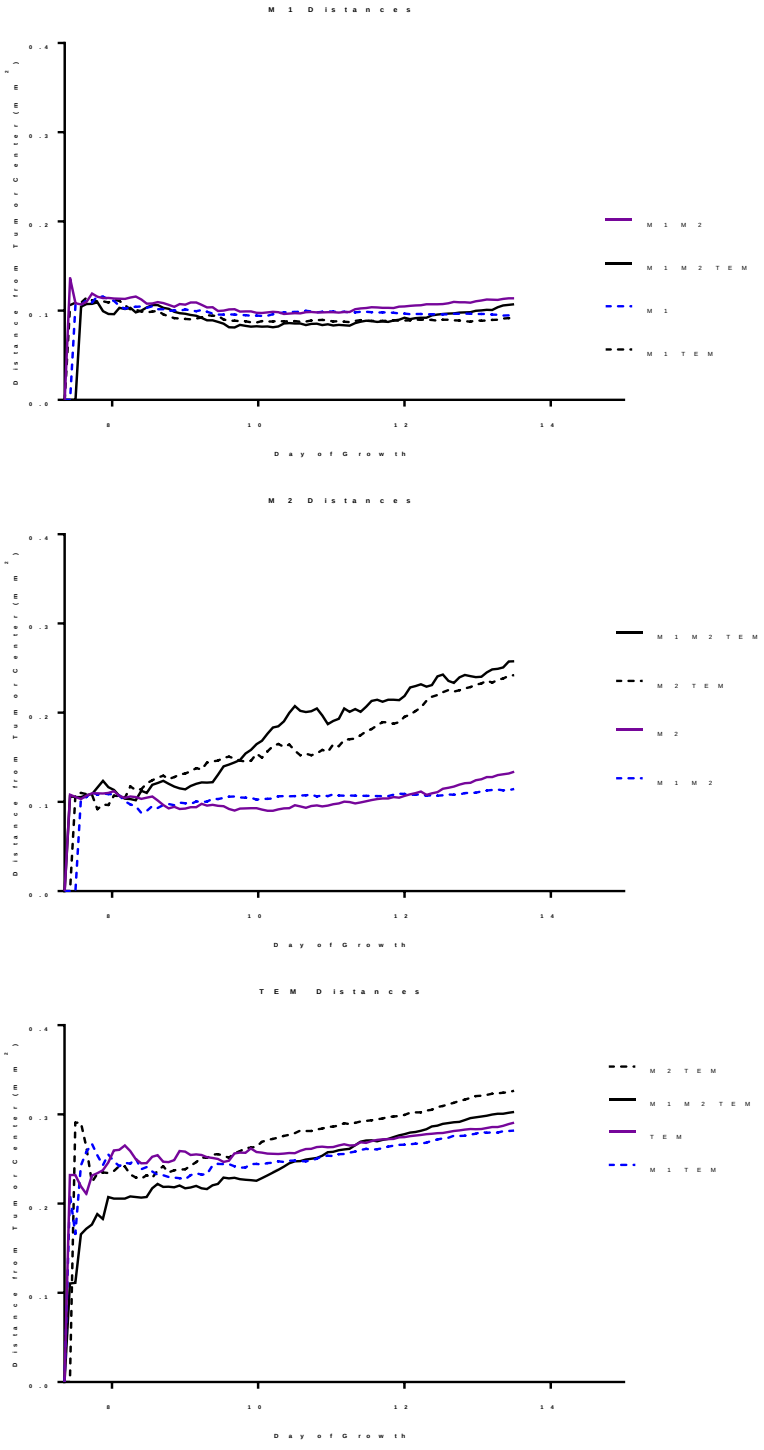

FIGURE 2 – MACROPHAGE DISTRIBUTIONS RELATIVE TO TUMOR

In variation 1, TIE2 expressing macrophages differentiating from the monocyte precursors became the majority subset in the tumor environment at 60.1%, matching *in vivo* data . In Variation 3 - M1 and M2 only - the M2/M1 ratio stabilized at 0.85. This ratio is half the median ratio for highly metastatic tumors, and within the normal range for more benign tumor populations (Cui 2013). A comparison of the two models shows that by modeling an increase in IL-10 in response to the IL-10 secreted by the TEMs, the M2/M1 ratio was shifted to 1.71 - a ratio consistent with more metastatic tumors (Cui 2013). The proportion of different macrophage types in time is shown in Fig. 3 and 4.

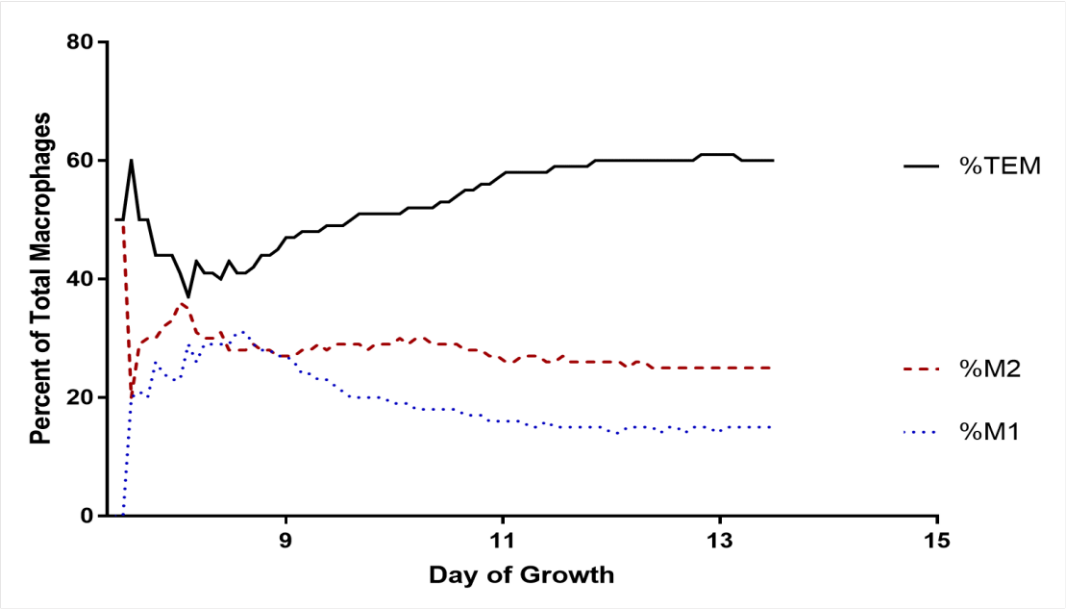

FIGURE 3 – MACROPHAGE RATIOS IN VARIATION 1

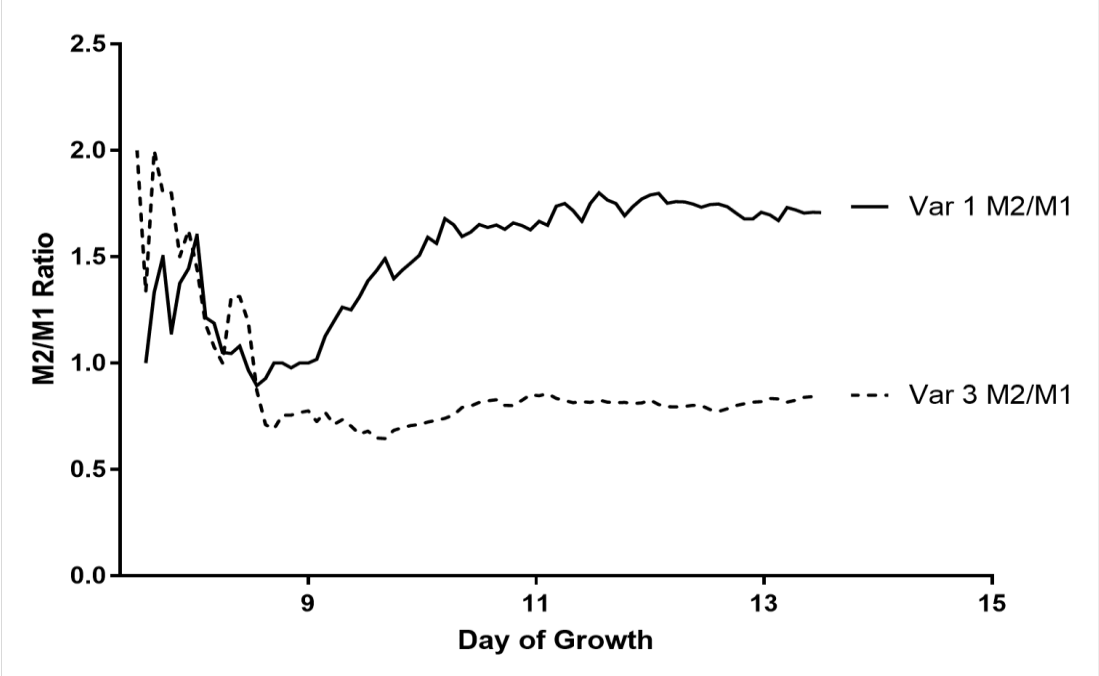

FIGURE 4 – MACROPHAGE RATIOS IN VARIATIONS 1 AND 3

C. Angiogenesis

Due to the protective clustering around angiogenic vasculature (see Fig. 1 middle right panel), variations with the TEM subtype displayed notably greater vascular development compared to the corresponding TEM-absent variations. Comparing variations 1 and 3, in which TEM is respectively present and ablated (Fig 5) a 3.81-fold increase in tumoral vasculature is observed, consistent with the nearly four-fold increase found by De Palma et al. in an analogous study *in* vivo (De Palma, Venneri et al.).

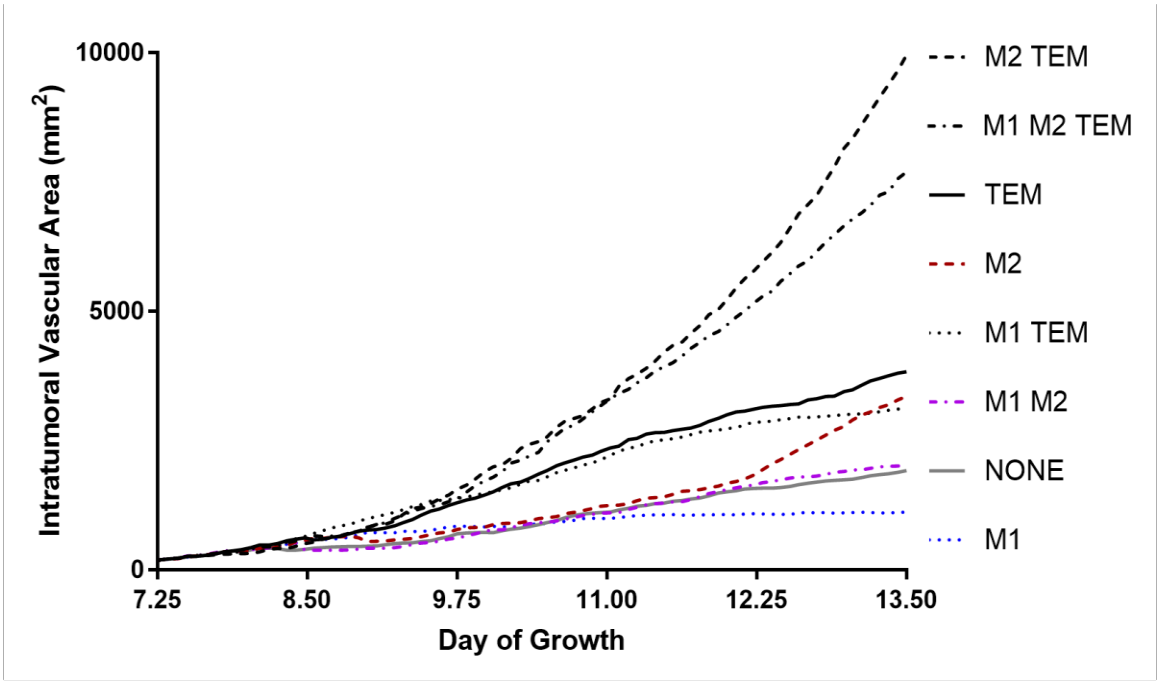

FIGURE 5 – INTRATUMORAL VASCULATURE BY VARIATION

As expected, variations with the TEM subtype present displayed greater vascular growth at the endpoint of the simulation, compared with those which did not. The presence of the M2 macrophage also encouraged vascular development, due to the increased size of the tumor achieved.

D. Tumor Radius

The effects of the TIE2 subtype on M1/M2 ratio and angiogenic protection in concert had a noticeable effect on the tumor progression (Fig. 6).

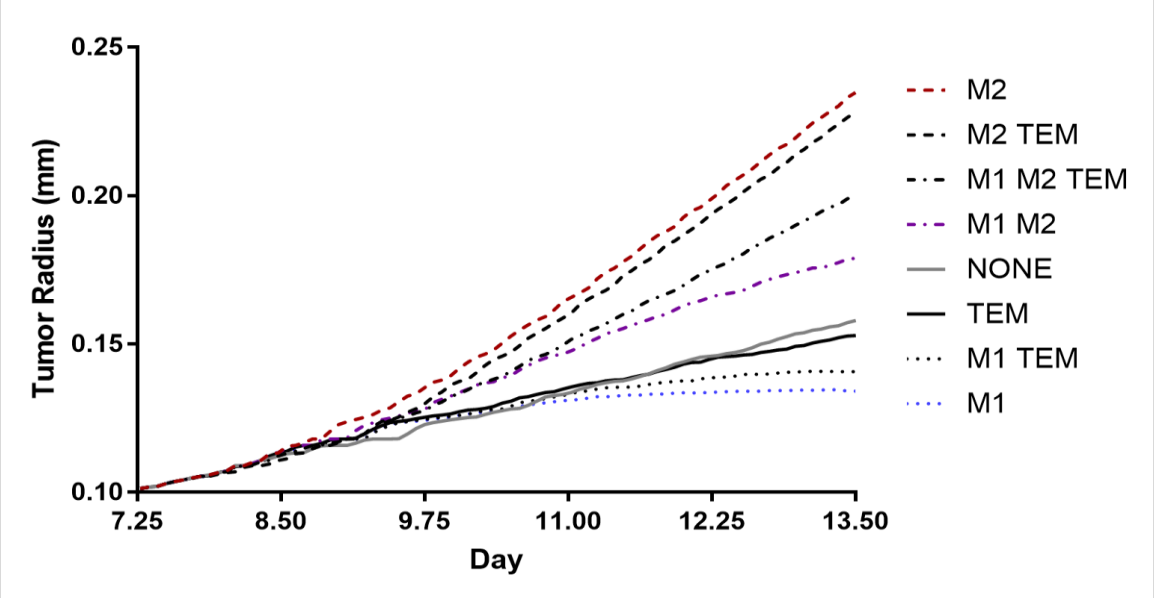

FIGURE 6 – TUMOR RADII BY VARIATION

Variation 1 with all three subtypes yielded an 11.9% increase in tumor radius over Variation 3, the TEM-ablated model, by the end of the simulation. The TEM-ablated variations showed a plateau in growth around Day 10. Variations 2 and 5, with TEM and M2, and M2 respectively, exhibited the strongest growth. This growth held steady to the end of the simulation, despite the development of hypoxic and necrotic regions within the tumor lesion (see Appendix IV). Variation 4, with M1 only, showed the least tumor growth, exhibiting a plateau consistent with findings of M1-only *in vivo* (Yuan, Hsiao et al.).

While all variations achieved a size that at least transiently rendered the interior portions hypoxic, only those with the TEM subtype and/or the M2 subtype were able to achieve continued growth through the end of the simulation (see Fig 6 and Fig 7). This

would indicate that the role of TEM in tumor vascularization mitigates an important immune-mediated check to unbounded tumoral growth.

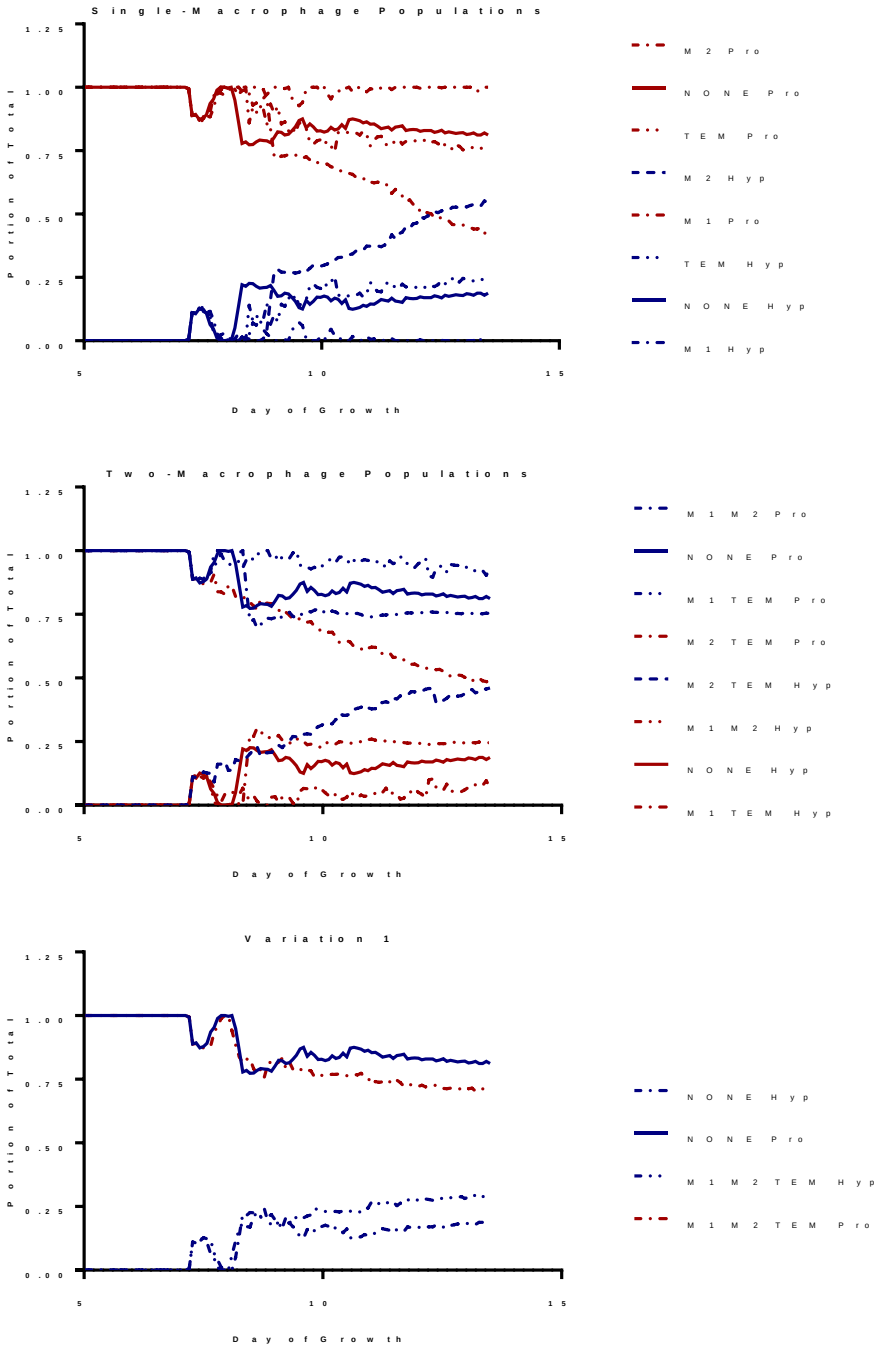

FIGURE 7 – PROLIFERATING AND HYPOXIC REGIONS

DISCUSSION

In this study, mathematical modeling was employed to explore the tumor-promoting and tumor-inhibiting roles of three major tumor-associated macrophage subtypes. A small metastatic lesion in the liver was simulated, growing in a highly-vascularized microenvironment, coupling the feedback between the tumor tissue, vasculature remodeling, and the macrophage activity. This work could provide a modeling platform for system analysis of the potent and varied effects of the macrophage activation spectrum on the tumor microenvironment, and presents the possibility of a valuable complement to current cancer therapy design. Given the ability of tumors to educate infiltrating macrophages to a tumorigenic subtype, methods of countering this may prevent the tumor from harnessing the body's most potent effectors of tissue remodeling as has been previously suggested (Quatromoni and Eruslanov 2012).

According to this paradigm, therapies which inhibit all monocytes and macrophages that infiltrate the tumor environment would be unideal, as they would fail to utilize the inherent tumoricidal activity of M1 macrophages. However, a more finessed approach by removal of the phenotypically and developmentally distinct TIE-2 expressing monocyte may be a more desirable and plausible target. Since this subset is

also implicated in the facilitation of cancer metastasis by degrading the ECM and guiding metastatic cells to the vasculature (e.g., as observed with breast cancer (Williams, Yeh et al. 2016)), blockade of this subtype from the tumor microenvironment may be a valuable target for both halting and reversing the metastatic progression of cancer in a patient (Venneri, Palma et al. 2007).

Additionally, the action of the TEM subtype may in part explain the pitfalls that have been observed in the use of VEGF inhibitors for tumor therapy (Vasudev and Reynolds 2014). In some instances, due to the tendency of inhibited tumoral blood supply to lead to increased tumor spread through fragmentation and migration of tumor cells, preventing the vasculature from growing towards the tumor could force a more malignant and metastatic phenotype, as has been observed experimentally (Rubenstein, Kim et al. 2000, Kunkel, Ulbricht et al. 2001, Lamszus, Kunkel et al. 2003, Pennacchietti, Michieli et al. 2003, Stockmann, Doedens et al. 2008, Ebos, Lee et al. 2009, Paez-Ribes, Allen et al. 2009, de Groot, Fuller et al. 2010), clinically (de Groot, Fuller et al. 2010, Sharpe, Stewart et al. 2013), and predicted by mathematical modeling (Cristini, Lowengrub et al. 2003, Cristini, Frieboes et al. 2005, Frieboes, Zheng et al. 2006, Wise, Lowengrub et al. 2008, Frieboes, Jin et al. 2010, Lowengrub, Frieboes et al. 2010).

Given that TEMs differentiate from a monocyte precursor distinct from the M1 and M2 subtypes, the possibility of TEM-specific therapies presents a promising method of fine-tuning the immune system's innate defense mechanisms without preventing the action of tumoricidal subtypes (Mantovani and Allavena 2015). This would educate the tumor to a more benign phenotype, rather than allowing it to alter the immune response to aid its malignancy.

RECOMMENDATIONS

Future work will explore the interaction of tumor and macrophage effects during treatment. Therapy could be delivered systemically as free drug or encapsulated in nanovectors, as previously simulated (Wu, Frieboes et al. 2014, Curtis, Wu et al. 2015, Curtis, England et al. 2016, Curtis, van Berkel et al. 2017), or its delivery to the tumor site could be targeted by tumor-associated macrophage uptake and release (Leonard, Curtis et al. 2016). Pharmaceutical ablation of tumor-promoting subtypes while supporting tumor-inhibiting phenotypes could provide further therapeutic options.

The combination of various modalities could be explored via the modeling framework presented herein, as such options would be difficult to evaluate solely through experimental observation. With input of patient tumor-specific information, such as size, vascularization, and macrophage density, this framework may in the longer term be of use to determine optimal therapy regimens leveraging the body's immune response to metastatic lesions.

REFERENCES

Beckebaum, S., X. Zhang, X. Chen, Z. Yu, A. Frilling, G. Dworacki, H. Grosse-Wilde, C. E. Broelsch, G. Gerken and V. R. Cicinnati (2004). "Increased levels of interleukin-10 in serum from patients with hepatocellular carcinoma correlate with profound numerical deficiencies and immature phenotype of circulating dendritic cell subsets." Clin Cancer Res **10**(21): 7260-7269.

Bocuk, D., P. Krause, S. Niebert, T. Pukrop, T. Beissbarth, M. Ghadimi and S. Koenig (2015). "Mouse models of colorectal and mammary cancer liver metastases and microenvironmental interplay with tumor-associated macrophages (TAMs)." Z Gastroenterol **53**(01): A4_34.

Byrne, H. M., S. M. Cox and C. E. Kelly (2004). "Macrophage-tumour interactions: In vivo dynamics." Discrete and Continuous Dynamical Systems - Series B **4**(1): 81-98.

Capone, F., E. Guerriero, A. Sorice, G. Colonna, G. Ciliberto and S. Costantini (2016). "Serum Cytokinome Profile Evaluation: A Tool to Define New Diagnostic and Prognostic Markers of Cancer Using Multiplexed Bead-Based Immunoassays." Mediators Inflamm **2016**: 3064643.

Catarinella, M., A. Monestiroli, G. Escobar, A. Fiocchi, N. L. Tran, R. Aiolfi, P. Marra, A. Esposito, F. Cipriani, L. Aldrighetti, M. Iannacone, L. Naldini, L. G. Guidotti and G. Sitia (2016). "IFNα gene/cell therapy curbs colorectal cancer colonization of the liver by acting on the hepatic microenvironment." EMBO Molecular Medicine **8**(2): 155-170.

Chanmee, T., P. Ontong, K. Konno and N. Itano (2014). "Tumor-Associated Macrophages as Major Players in the Tumor Microenvironment." Cancers **6**(3): 1670-1690.

Chen, D., A. A. Bobko, A. C. Gross, R. Evans, C. B. Marsh, V. V. Khramtsov, T. D. Eubank and A. Friedman (2014). "Involvement of tumor macrophage HIFs in chemotherapy effectiveness: Mathematical modeling of oxygen, pH, and glutathione." PLoS ONE **9**(10).

Coffelt, S. B., Y. Y. Chen, M. Muthana, A. F. Welford, A. O. Tal, A. Scholz, K. H. Plate, Y. Reiss, C. Murdoch, M. De Palma and C. E. Lewis (2011). "Angiopoietin 2 stimulates

TIE2-expressing monocytes to suppress T cell activation and to promote regulatory T cell expansion." J Immunol **186**(7): 4183-4190.

Coffelt, S. B., A. O. Tal, A. Scholz, M. De Palma, S. Patel, C. Urbich, S. K. Biswas, C. Murdoch, K. H. Plate, Y. Reiss and C. E. Lewis (2010). "Angiopoietin-2 Regulates Gene Expression in TIE2-Expressing Monocytes and Augments Their Inherent Proangiogenic Functions." Cancer Research **70**(13): 5270-5280.

Cristini, V., H. B. Frieboes, R. Gatenby, S. Caserta, M. Ferrari and J. Sinek (2005). "Morphologic instability and cancer invasion." Clin Cancer Res **11**(19 Pt 1): 6772-6779.

Cristini, V., J. Lowengrub and Q. Nie (2003). "Nonlinear simulation of tumor growth." J Math Biol **46**(3): 191-224.

Cui, Y.-L. L., Hui-Kai; Zhou, Hong-Yuan; Zhang, Ti; Li, Qiang; (2013). "Correlations of Tumor-associated Macrophage Subtypes with Liver Metastases of Colorectal Cancer." Asian Pacific Journal of Cancer Prevention **14**(2): 1003-1007.

Cui, Y.-L. L., Hui-Kai; Zhou, Hong-Yuan; Zhang, Ti; Li, Qiang; (2013). "Correlations of Tumor-associated Macrophage Subtypes with Liver Metastases of Colorectal Cancer." Asian Pacific Journal of Cancer Prevention **14**(2): 1003-1007.

Curtis, L. T., C. G. England, M. Wu, J. Lowengrub and H. B. Frieboes (2016). "An interdisciplinary computational/experimental approach to evaluate drug-loaded gold nanoparticle tumor cytotoxicity." Nanomedicine (Lond) **11**(3): 197-216.

Curtis, L. T., V. H. van Berkel and H. B. Frieboes (2017). "Intracellular modeling of multiple-drug regimens for lung cancer chemotherapy." Pharmacological Research **(in press)**.

Curtis, L. T., M. Wu, J. Lowengrub, P. Decuzzi and H. B. Frieboes (2015). "Computational Modeling of Tumor Response to Drug Release from Vasculature-Bound Nanoparticles." PLoS One **10**(12): e0144888.

de Groot, J. F., G. Fuller, A. J. Kumar, Y. Piao, K. Eterovic, Y. Ji and C. A. Conrad (2010). "Tumor invasion after treatment of glioblastoma with bevacizumab: radiographic and pathologic correlation in humans and mice." Neuro Oncol **12**(3): 233-242.

De Palma, M. and C. E. Lewis (2013). "Macrophage regulation of tumor responses to anticancer therapies." Cancer Cell **23**(3): 277-286.

De Palma, M., C. Murdoch, M. A. Venneri, L. Naldini and C. E. Lewis (2007). "Tie2-expressing monocytes: regulation of tumor angiogenesis and therapeutic implications." Trends in Immunology **28**(12): 519-524.

De Palma, M. and L. Naldini (2011). "Angiopoietin-2 TIEs Up Macrophages in Tumor Angiogenesis." Clinical Cancer Research **17**(16): 5226-5232.

De Palma, M., M. A. Venneri, R. Galli, L. S. Sergi, L. S. Politi, M. Sampaolesi and L. Naldini (2008). "Tie2 identifies a hematopoietic lineage of proangiogenic monocytes required for tumor vessel formation and a mesenchymal population of pericyte progenitors." Cancer Cell **8**(3): 211-226.

Dehqanzada, Z. A., C. E. Storrer, M. T. Hueman, R. J. Foley, K. A. Harris, Y. H. Jama, C. D. Shriver, S. Ponniah and G. E. Peoples (2007). "Assessing serum cytokine profiles in breast cancer patients receiving a HER2/neu vaccine using Luminex technology." Oncol Rep **17**(3): 687-694.

Ebos, J. M., C. R. Lee, W. Cruz-Munoz, G. A. Bjarnason, J. G. Christensen and R. S. Kerbel (2009). "Accelerated metastasis after short-term treatment with a potent inhibitor of tumor angiogenesis." Cancer Cell **15**(3): 232-239.

Edin, S., M. L. Wikberg, A. M. Dahlin, J. Rutegård, Å. Öberg, P.-A. Oldenborg and R. Palmqvist (2012). "The Distribution of Macrophages with a M1 or M2 Phenotype in Relation to Prognosis and the Molecular Characteristics of Colorectal Cancer." PLoS ONE **7**(10): e47045.

Esquivel-Velazquez, M., P. Ostoa-Saloma, M. I. Palacios-Arreola, K. E. Nava-Castro, J. I. Castro and J. Morales-Montor (2015). "The role of cytokines in breast cancer development and progression." J Interferon Cytokine Res **35**(1): 1-16.

Frieboes, H. B., F. Jin, Y. L. Chuang, S. M. Wise, J. S. Lowengrub and V. Cristini (2010). "Three-dimensional multispecies nonlinear tumor growth-II: Tumor invasion and angiogenesis." J Theor Biol **264**(4): 1254-1278.

Frieboes, H. B., X. Zheng, C. H. Sun, B. Tromberg, R. Gatenby and V. Cristini (2006). "An integrated computational/experimental model of tumor invasion." Cancer Res **66**(3): 1597-1604.

Guo, C., A. Buranych, D. Sarkar, P. B. Fisher and X. Y. Wang (2013). "The role of tumor-associated macrophages in tumor vascularization." Vasc Cell **5**(1): 20.

Guo, C., A. Buranych, D. Sarkar, P. B. Fisher and X. Y. Wang (2014). "Correction: The role of tumor-associated macrophages in tumor vascularization." Vasc Cell **6**(1): 2.

Hamidullah, B. Changkija and R. Konwar (2012). "Role of interleukin-10 in breast cancer." Breast Cancer Res Treat **133**(1): 11-21.

Hsu, C.-W., R. A. Poché, J. E. Saik, S. Ali, S. Wang, N. Yosef, G. A. Calderon, L. Scott, Jr., T. J. Vadakkan, I. V. Larina, J. L. West and M. E. Dickinson (2015). "Improved Angiogenesis in Response to Localized Delivery of Macrophage-Recruiting Molecules." PLOS ONE **10**(7): e0131643.

Italiani, P. and D. Boraschi (2014). "From Monocytes to M1/M2 Macrophages: Phenotypical vs. Functional Differentiation." Frontiers in Immunology **5**: 514.

Kim, O.-H., G.-H. Kang, H. Noh, J.-Y. Cha, H.-J. Lee, J.-H. Yoon, M. Mamura, J.-S. Nam, D. H. Lee, Y. A. Kim, Y. J. Park, H. Kim and B.-C. Oh (2013). "Proangiogenic TIE2(+)/CD31(+) Macrophages Are the Predominant Population of Tumor-Associated Macrophages Infiltrating Metastatic Lymph Nodes." Molecules and Cells **36**(5): 432-438.

Kozlowski, L., I. Zakrzewska, P. Tokajuk and M. Z. Wojtukiewicz (2003). "Concentration of interleukin-6 (IL-6), interleukin-8 (IL-8) and interleukin-10 (IL-10) in blood serum of breast cancer patients." Rocz Akad Med Bialymst **48**: 82-84.

Kunkel, P., U. Ulbricht, P. Bohlen, M. A. Brockmann, R. Fillbrandt, D. Stavrou, M. Westphal and K. Lamszus (2001). "Inhibition of glioma angiogenesis and growth in vivo by systemic treatment with a monoclonal antibody against vascular endothelial growth factor receptor-2." Cancer Res **61**(18): 6624-6628.

Lamszus, K., P. Kunkel and M. Westphal (2003). "Invasion as limitation to anti-angiogenic glioma therapy." Acta Neurochir Suppl **88**: 169-177.

Laoui, D., K. Movahedi, E. Van Overmeire, J. Van den Bossche, E. Schouppe, C. Mommer, A. Nikolaou, Y. Morias, P. De Baetselier and J. A. Van Ginderachter (2011). "Tumor-associated macrophages in breast cancer: distinct subsets, distinct functions." Int J Dev Biol **55**(7-9): 861-867.

Leonard, F., L. T. Curtis, P. Yesantharao, T. Tanei, J. F. Alexander, M. Wu, J. Lowengrub, X. Liu, M. Ferrari, K. Yokoi, H. B. Frieboes and B. Godin (2016). "Enhanced performance of macrophage-encapsulated nanoparticle albumin-bound-paclitaxel in hypo-perfused cancer lesions." Nanoscale **8**(25): 12544-12552.

Lewis, C. and C. Murdoch (2005). "Macrophage Responses to Hypoxia : Implications for Tumor Progression and Anti-Cancer Therapies." The American Journal of Pathology **167**(3): 627-635.

Lewis, C. E., M. De Palma and L. Naldini (2007). "Tie2-Expressing Monocytes and Tumor Angiogenesis: Regulation by Hypoxia and Angiopoietin-2." Cancer Research **67**(18): 8429-8432.

Lowengrub, J. S., H. B. Frieboes, F. Jin, Y. L. Chuang, X. Li, P. Macklin, S. M. Wise and V. Cristini (2010). "Nonlinear modelling of cancer: bridging the gap between cells and tumours." Nonlinearity **23**(1): R1-R9.

Macklin, P. and J. Lowengrub (2007). "Nonlinear simulation of the effect of microenvironment on tumor growth." J Theor Biol **245**(4): 677-704.

Macklin, P. and J. S. Lowengrub (2008). "A New Ghost Cell/Level Set Method for Moving Boundary Problems: Application to Tumor Growth." Journal of scientific computing **35**(2-3): 266-299.

Macklin, P., S. McDougall, A. R. A. Anderson, M. A. J. Chaplain, V. Cristini and J. Lowengrub (2009). "Multiscale modelling and nonlinear simulation of vascular tumour growth." Journal of mathematical biology **58**(4-5): 765-798.

Mantovani, A. and P. Allavena (2015). "The interaction of anticancer therapies with tumor-associated macrophages." The Journal of Experimental Medicine **212**(4): 435-445.

Matsubara, T., T. Kanto, S. Kuroda, S. Yoshio, K. Higashitani, N. Kakita, M. Miyazaki, M. Sakakibara, N. Hiramatsu, A. Kasahara, Y. Tomimaru, A. Tomokuni, H. Nagano, N. Hayashi and T. Takehara (2013). "TIE2-expressing monocytes as a diagnostic marker for hepatocellular carcinoma correlates with angiogenesis." Hepatology **57**(4): 1416-1425.

Mazzieri, R., F. Pucci, D. Moi, E. Zonari, A. Ranghetti, A. Berti, L. S. Politi, B. Gentner, J. L. Brown, L. Naldini and M. De Palma (2011). "Targeting the ANG2/TIE2 axis inhibits tumor growth and metastasis by impairing angiogenesis and disabling rebounds of proangiogenic myeloid cells." Cancer Cell **19**(4): 512-526.

McDougall, S. R., A. R. Anderson and M. A. Chaplain (2006). "Mathematical modelling of dynamic adaptive tumour-induced angiogenesis: clinical implications and therapeutic targeting strategies." J Theor Biol **241**(3): 564-589.

McDougall, S. R., A. R. Anderson, M. A. Chaplain and J. A. Sherratt (2002). "Mathematical modelling of flow through vascular networks: implications for tumour-induced angiogenesis and chemotherapy strategies." Bull Math Biol **64**(4): 673-702.

McDougall, S. R., A. R. A. Anderson and M. A. J. Chaplain (2006). "Mathematical modelling of dynamic adaptive tumour-induced angiogenesis: Clinical implications and therapeutic targeting strategies." Journal of Theoretical Biology **241**(3): 564-589.

Mocellin, S., F. M. Marincola and H. A. Young (2005). "Interleukin-10 and the immune response against cancer: a counterpoint." J Leukoc Biol **78**(5): 1043-1051.

Murdoch, C., A. Giannoudis and C. E. Lewis (2004). "Mechanisms regulating the recruitment of macrophages into hypoxic areas of tumors and other ischemic tissues." Blood **104**(8): 2224.

Nugent, L. J. and R. K. Jain (1984). "Extravascular diffusion in normal and neoplastic tissues." Cancer Research **44**(1): 238-244.

Owen, M. R., H. M. Byrne and C. E. Lewis (2004). "Mathematical modelling of the use of macrophages as vehicles for drug delivery to hypoxic tumour sites." Journal of Theoretical Biology **226**(4): 377-391.

Owen, M. R. and J. A. Sherratt (1998). "Modelling the macrophage invasion of turnours: Effects on growth and composition." IMA J. Math. Appl. Med. **15**(2): 165-185.

Owen, M. R. and J. A. Sherratt (1999). "Mathematical modelling of macrophage dynamics in tumours." Math. Mod. Meth. Appl. S. **9**(4): 513-539.

Owen, M. R., I. J. Stamper, M. Muthana, G. W. Richardson, J. Dobson, C. E. Lewis and H. M. Byrne (2011). "Mathematical modeling predicts synergistic antitumor effects of combining a macrophage-based, hypoxia-targeted gene therapy with chemotherapy." Cancer Research **71**(8): 2826-2837.

Paez-Ribes, M., E. Allen, J. Hudock, T. Takeda, H. Okuyama, F. Vinals, M. Inoue, G. Bergers, D. Hanahan and O. Casanovas (2009). "Antiangiogenic therapy elicits malignant progression of tumors to increased local invasion and distant metastasis." Cancer Cell **15**(3): 220-231.

Patel, A. S., A. Smith, S. Nucera, D. Biziato, P. Saha, R. Q. Attia, J. Humphries, K. Mattock, S. P. Grover, O. T. Lyons, L. G. Guidotti, R. Siow, A. Ivetic, S. Egginton, M. Waltham, L. Naldini, M. De Palma and B. Modarai (2013). "TIE2-expressing monocytes/macrophages regulate revascularization of the ischemic limb." EMBO Molecular Medicine **5**(6): 858-869.

Pennacchietti, S., P. Michieli, M. Galluzzo, M. Mazzone, S. Giordano and P. M. Comoglio (2003). "Hypoxia promotes invasive growth by transcriptional activation of the met protooncogene." Cancer Cell **3**(4): 347-361.

Plank, M. J. and B. D. Sleeman (2003). "Tumour-Induced Angiogenesis: A Review." Journal of Theoretical Medicine **5**(3-4): 137-153.

Pries, A. R., M. Hopfner, F. le Noble, M. W. Dewhirst and T. W. Secomb (2010). "The shunt problem: control of functional shunting in normal and tumour vasculature." Nat Rev Cancer **10**(8): 587-593.

Pries, A. R., T. W. Secomb and P. Gaehtgens (1998). "Structural adaptation and stability of microvascular networks: theory and simulations." Am J Physiol **275**(2 Pt 2): H349-360.

Quatromoni, J. G. and E. Eruslanov (2012). "Tumor-associated macrophages: function, phenotype, and link to prognosis in human lung cancer." American Journal of Translational Research **4**(4): 376-389.

Riabov, V., A. Gudima, N. Wang, A. Mickley, A. Orekhov and J. Kzhyshkowska (2014). "Role of tumor associated macrophages in tumor angiogenesis and lymphangiogenesis." Front Physiol **5**: 75.

Roca, H., Z. S. Varsos, S. Sud, M. J. Craig, C. Ying and K. J. Pienta (2009). "CCL2 and Interleukin-6 Promote Survival of Human CD11b(+) Peripheral Blood Mononuclear Cells and Induce M2-type Macrophage Polarization." The Journal of Biological Chemistry **284**(49): 34342-34354.

Rubenstein, J. L., J. Kim, T. Ozawa, M. Zhang, M. Westphal, D. F. Deen and M. A. Shuman (2000). "Anti-VEGF antibody treatment of glioblastoma prolongs survival but results in increased vascular cooption." Neoplasia **2**(4): 306-314.

Sharpe, K., G. D. Stewart, A. Mackay, C. Van Neste, C. Rofe, D. Berney, I. Kayani, A. Bex, E. Wan, F. C. O'Mahony, M. O'Donnell, S. Chowdhury, R. Doshi, C. Ho-Yen, M. Gerlinger, D. Baker, N. Smith, B. Davies, A. Sahdev, E. Boleti, T. De Meyer, W. Van Criekinge, L. Beltran, Y. J. Lu, D. J. Harrison, A. R. Reynolds and T. Powles (2013). "The effect of VEGF-targeted therapy on biomarker expression in sequential tissue from patients with metastatic clear cell renal cancer." Clin Cancer Res **19**(24): 6924-6934.

Sica, A. and A. Mantovani "Macrophage plasticity and polarization: in vivo veritas." The Journal of Clinical Investigation **122**(3): 787-795.

Squadrito, M. L. and M. De Palma (2011). "Macrophage regulation of tumor angiogenesis: implications for cancer therapy." Mol Aspects Med **32**(2): 123-145.

Stockmann, C., A. Doedens, A. Weidemann, N. Zhang, N. Takeda, J. I. Greenberg, D. A. Cheresh and R. S. Johnson (2008). "Deletion of vascular endothelial growth factor in myeloid cells accelerates tumorigenesis." Nature **456**(7223): 814-818.

Stockmann, C., D. Schadendorf, R. Klose and I. Helfrich (2014). "The impact of the immune system on tumor: angiogenesis and vascular remodeling." Front Oncol **4**: 69.

Tripathi, C., B. N. Tewari, R. K. Kanchan, K. S. Baghel, N. Nautiyal, R. Shrivastava, H. Kaur, M. L. Bhatt and S. Bhadauria (2014). "Macrophages are recruited to hypoxic tumor areas and acquire a pro-angiogenic M2-polarized phenotype via hypoxic cancer cell derived cytokines Oncostatin M and Eotaxin." Oncotarget **5**(14): 5350-5368.

van de Ven, A. L., M. Wu, J. Lowengrub, S. R. McDougall, M. A. Chaplain, V. Cristini, M. Ferrari and H. B. Frieboes (2012). "Integrated intravital microscopy and mathematical modeling to optimize nanotherapeutics delivery to tumors." AIP Adv **2**(1): 11208.

Vasudev, N. S. and A. R. Reynolds (2014). "Anti-angiogenic therapy for cancer: current progress, unresolved questions and future directions." Angiogenesis **17**(3): 471-494.

Venneri, M. A., M. D. Palma, M. Ponzoni, F. Pucci, C. Scielzo, E. Zonari, R. Mazzieri, C. Doglioni and L. Naldini (2007). "Identification of proangiogenic TIE2-expressing monocytes (TEMs) in human peripheral blood and cancer." Blood **109**(12): 5276-5285.

Webb, S. D., M. R. Owen, H. M. Byrne, C. Murdoch and C. E. Lewis (2007). "Macrophage-based anti-cancer therapy: Modelling different modes of tumour targeting." Bulletin of Mathematical Biology **69**(5): 1747-1776.

Welford, A. F., D. Biziato, S. B. Coffelt, S. Nucera, M. Fisher, F. Pucci, C. Di Serio, L. Naldini, M. De Palma, G. M. Tozer and C. E. Lewis (2011). "TIE2-expressing macrophages limit the therapeutic efficacy of the vascular-disrupting agent combretastatin A4 phosphate in mice." J Clin Invest **121**(5): 1969-1973.

Williams, C. B., E. S. Yeh and A. C. Soloff (2016). "Tumor-associated macrophages: unwitting accomplices in breast cancer malignancy." NPJ breast cancer **2**: 15025.

Wise, S. M., J. S. Lowengrub, H. B. Frieboes and V. Cristini (2008). "Three-dimensional multispecies nonlinear tumor growth--I Model and numerical method." J Theor Biol **253**(3): 524-543.

Wu, M., H. B. Frieboes, M. A. Chaplain, S. R. McDougall, V. Cristini and J. S. Lowengrub (2014). "The effect of interstitial pressure on therapeutic agent transport: coupling with the tumor blood and lymphatic vascular systems." J Theor Biol **355**: 194-207.

Wu, M., H. B. Frieboes, S. R. McDougall, M. A. J. Chaplain, V. Cristini and J. Lowengrub (2013). "The effect of interstitial pressure on tumor growth: Coupling with the blood and lymphatic vascular systems." Journal of Theoretical Biology **320**: 131-151.

Yuan, A., Y.-J. Hsiao, H.-Y. Chen, H.-W. Chen, C.-C. Ho, Y.-Y. Chen, Y.-C. Liu, T.-H. Hong, S.-L. Yu, J. J. W. Chen and P.-C. Yang (2015). "Opposite Effects of M1 and M2 Macrophage Subtypes on Lung Cancer Progression." Scientific Reports **5**: 14273.